Electron Ejection from Ta by He^+, He^{++}, and He_2^+

HOMER D. HAGSTRUM
Bell Telephone Laboratories, Murray Hill, New Jersey
(Received April 2, 1953)

Measurements of total yield (γ_i) and kinetic energy distribution are reported for electrons ejected from tantalum by the ions He^+, He^{++}, and He_2^+ in the kinetic energy range 10 to 1000 ev. The evidence presented indicates that the electrons are released by a collision of the second kind of the ion with the metal surface (potential ejection). One internal secondary electron is produced per incident ion. The probability of this electron escaping is reduced by the possibility of internal reflection at the image barrier at the metal surface. γ_i for the slowest ions is observed to be 0.14, 0.52, and 0.10 for He^+, He^{++}, and He_2^+, respectively. The data presented must be considered representative of gas-covered tantalum, since no gas was observed to desorb from the target on heating to 1750°K. γ_i was found not to vary with time after cooling the target indicating rapid re-establishment of the equilibrium gas layer on the surface from within the metal. The work function of the covered Ta surface is found to be *ca* 4.9 ev, some 0.8 ev higher than that of atomically clean Ta. Considerations based on a theory which includes variation of energy levels near the metal surface show resonance neutralization of He^+ at the covered Ta surface not to be possible. Thus only the so-called direct process of potential ejection occurs, with which conclusion the measured energy limits of ejected electrons are in agreement.

I. INTRODUCTION

THE work reported in this paper is part of a program of study of electron ejection from the refractory metals by noble gas ions. Reports of work on electron ejection from Mo by He^+, He^{++}, and He_2^+ ions[1] and of the instrumentation and method[2] have been published. In these papers experimental apparatus and procedure, as well as the theoretical predictions concerning the so-called potential ejection of electrons by ions based on published theoretical treatments, have been discussed in some detail. Frequent reference to these discussions are made throughout this paper.

Measurements reported here include those of total electron yield (γ_i) *versus* incident ion kinetic energy in the range 10 to 1000 ev for He^+, He^{++}, and He_2^+, and of electron energy distributions for incident He^+ and He^{++} ions (Sec. III). It has been a primary goal in the present series of studies of electron ejection by ions to make these measurements with atomically clean target surfaces. Tantalum presents an interesting problem in this regard. The evidence is that, on heating the tantalum to 1750°K, the equilibrium adsorbed gas layer is absorbed into the lattice, and that the surface layer is re-established from within the metal rapidly on cooling. The work function of the cold tantalum appears to be some 0.8 ev higher than that of the hot tantalum. These conclusions are demanded by the observations of contact potential, energy limits of ejected electrons, electron yield as a function of time after cooling the target, and the adsorption rate of molecules from the surrounding residual gases in the apparatus (Sec. IV).

A brief sketch of an extension of the theory of potential ejection is given in this paper (Sec. V). In this theory an attempt is made to include the energies of interaction between the metal and the atomic particle (ion, metastable atom, normal atom) outside its surface. Electronic transitions which can occur as the ion approaches the metal surface are then described as transitions, obeying the Franck-Condon principle, between suitable potential energy curves. Only those aspects peculiar to the tantalum case are discussed in any detail here. A complete presentation of the theory is in preparation for separate publication. It should also be mentioned that these theoretical ideas and hence their application in the case of tantalum are strongly supported by experimental work with singly and multiply charged ions from all the noble gases (He, Ne, Ar, Kr, Xe) on atomically clean tungsten. This work has also been completed and is in preparation for publication.

In view of previous publications,[1,2] only a brief statement concerning apparatus and general procedure is included here (Sec. II). Notation used in this paper is defined in Table I in which numerical values used are also specified.

II. EXPERIMENTAL APPARATUS AND PROCEDURE

The experiment was performed with an apparatus in which ions, formed by electron impact, are (m/e)-analyzed and focused by suitable ion lenses on the front surface of a ribbon target situated in the center of a spherical electron collector. This instrument is that used in the molybdenum work[1] and is the first of the series discussed in the report on instrumentation and procedure.[2] The experimental method and evacuation procedure were the same as those used in the study of molybdenum[1] with the modifications noted below.

A conventional ionization manometer (the D.P.I. Model VG-1A) was used.[3] It read 1 to 2×10^{-8} mm Hg during the experiment. This is now recognized to be the lowest apparent pressure reading attainable with such a gauge, the plate current then actually resulting primarily from the release of photoelectrons by soft x-rays generated at the grid. That the pressure conditions were comparable to those of the molybdenum

[1] H. D. Hagstrum, Phys. Rev. **89**, 244 (1953).
[2] H. D. Hagstrum, submitted for publication in *The Review of Scientific Instruments*.
[3] The Bayard-Alpert ionization manometer [R. T. Bayard and D. Alpert, Rev. Sci. Instr. **21**, 571 (1950)] was disclosed during the course of the present experiments.

TABLE I. Notation and numerical values used.

e^-	electron
$e^-_{Ta}(-\alpha)$	electron in conduction band of Ta, α ev below top of surface barrier
e	electronic charge
He	normal helium atom
He*	excited helium atom
He^m	^3S metastable helium atom
He^+, He^{++}	atomic helium ions
He_2^+	diatomic molecular helium ion
E_i(He), E_i, E_{i1}	first ionization energy of He ($\rightarrow He^+$; =24.58 ev)[a]
E_{i2}(He), E_{i2}	second ionization energy of He ($\rightarrow He^{++}$; $=E_{i1}$(He)$+E_{i1}$(He^+)=78.98 ev)[a]
E_i^v(He_2), E_i^v	vertical ionization energy of He_2 ($\rightarrow He^+$; $\cong$16.8 ev)[b]
$E_x(He^m)$	electronic excitation energy of He^m (=19.81 ev)[a]
ϵ	ionization energy of He^m ($\rightarrow He^+$; $=E_i(He^m)=E_i$(He)$-E_x$(He)=4.77 ev)
$E_k(e^-)$, $E_k(He^+)$	kinetic energy of e^- and He^+, respectively
φ(Ta), φ	work function of atomically clean tantalum (=4.12 ev)[c]
φ_h	work function of hot target during contact potential determination (taken in this work to be φ(Ta)=4.12 ev)
φ_c	work function of target at room temperature
W_i(Ta), W_i	width of filled portion of conduction band in tantalum ($\cong$5.4 ev)[d]
W_a(Ta), W_a	$W_i+\varphi$ (for the cold target $W_i+\varphi_c$ should be used)
$E(He^+-Ta)$	energy of interaction of He^+ with the Ta target
$E(He^m-Ta)$	energy of interaction of He^m with the Ta target
α_n	static polarizability of He (2.16×10^{-25} cm^3)[e]
α_m	static polarizability of He^m (*ca* 57×10^{-25} cm^3)[f]
k_{max}	wave number of an electron in the highest occupied state in the metal (*ca* 10^8 cm^{-1})[g]
S, T	electrode designations for electron collector and target, respectively
V_{ST}	voltage between S and T (positive when T is positive with respect to S; in this work corrected for contact potential with respect to the hot target)
V_r	true retarding potential V_{ST}, corrected for contact potential with respect to the cold target
I_S, I_T	positive currents to electrodes S and T, respectively
I^i	primary ion current entering electrode S
I_r	current flowing between S and T when electron current ejected from T is suppressed, i.e., total current which flows as a result of reflection at T of incident ions as ions or metastable atoms and electron ejection by these particles at S. (See Fig. 4 of reference 1)
γ_i	number of electrons ejected at T per incident ion
ρ	$I_S/(I_T+I_S)$ ($=-\gamma_i$ for $V_r\ll0$)
R	ρ at $V_r\gg0$ ($=I_r/I^i$)
z	number of electronic charges per ion
$zd\rho/dV_r$	electron energy distribution function
p	pressure in mm Hg
Δt_c	target cold interval (measured from instant target is cooled after a flash)
Δt_h	target hot interval (measured from instant heating current is turned on)
Δt_m	monolayer adsorption time (Δt_c required to reach the surface condition at which the adsorption rate is observed to decrease from a relatively high to a relatively low value)
$(\Delta p)_1$	pressure rise observed at $\Delta t_h\cong1$ sec resulting from desorption at the target
$(\Delta p)_2$	pressure rise observed at $\Delta t_h\cong30$ sec resulting from desorption at the target supporting leads

[a] C. E. Moore, *Atomic Energy Levels*, National Bureau of Standards Circular 467 (U. S. Government Printing Office, Washington, D. C., 1949), Vol. 1. Note that ionization energies are designated E_i rather than I, as in reference 1, to avoid confusion with currents. Excitation energy is denoted by E_x rather than E_e.

[b] This is taken to be the energy liberated accompanying neutralization by transition from the stable He_2^+ state to the repulsive He_2 state at constant nuclear separation. The value given here is that quoted by R. Meyerott, Phys. Rev. **70**, 671 (1946), based on observations of O. S. Duffendack and H. L. Smith, Phys. Rev. **34**, 68 (1929) of spectral enhancement in the $A^2\Pi\rightarrow X^2\Sigma$ system of CO^+ by the molecular ion He_2^+.

[c] H. B. Michaelson, J. Appl. Phys. **21**, 536 (1950).

[d] M. F. Manning and M. I. Chodorow, Phys. Rev. **56**, 787 (1939).

[e] *Landolt-Börnstein Tables* (Verlag Julius Springer, Berlin, 1950), Vol. I, Part I, p. 401.

[f] This value has been estimated on the basis of the one-term formula for the static polarizability given by H. Margenau, Revs. Modern Phys. **11**, 1 (1939), Eq. (C9). The f values for He and He^m are taken to be equal and the Δ values as equal to the corresponding E_i. Thus,

$$\alpha_m\cong[E_i(\text{He})/E_i(\text{He}^m)]^2\cdot\alpha_n=57\times10^{25}\text{ cm}^3.$$

[g] This value is estimated from Fig. 3 of Manning and Chodorow (footnote d) for an electron at the highest occupied level in the metal Ta, 5.4 ev above the bottom of the conduction band.

experiment can be judged from the measurement of the rate of adsorption by the target support leads (see Sec. IV and Fig. 9). The 20 percent increase in initial slope of the $(\Delta p)_2$ *vs* Δt_c curve of Fig. 9, observed when He gas was admitted to the apparatus, indicates the admission of only a very small amount of adsorbable impurity with the He.[1]

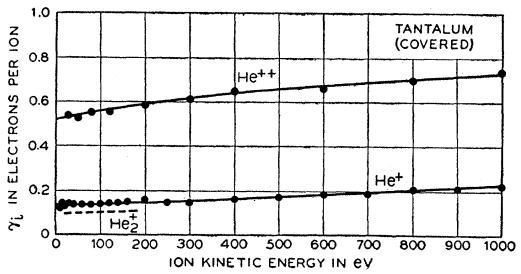

FIG. 1. Plots of total electron yield γ_i, as a function of ion kinetic energy for He^+, He^{++}, and He_2^+. The data must be taken as representative of gas-covered tantalum, as is discussed in the text.

III. RESULTS OF ELECTRON EJECTION EXPERIMENTS

The variation of total yield (γ_i) with ion kinetic energy has been determined for each of the ions He^+, He^{++}, and He_2^+. Results are plotted in Fig. 1. The He_2^+ ions were formed in the ionization chamber at relatively high gas pressure by the two-stage process: $He+e^-\rightarrow He^*+e^-$, followed by: $He^*+He\rightarrow He_2^++e^-$.[4] Beam currents of this ion were small; the data scatter is about ±30 percent about the He_2^+ line in Fig. 4. Measurements for He^+ and He^{++} are believed to be accurate to 5 percent.

It will be noted that the data of Fig. 1 are attributed to "covered" tantalum. This is meant to call attention to the fact that the tantalum surface is not atomically

[4] J. A. Hornbeck and J. P. Molnar, Phys. Rev. **84**, 621 (1951).

clean in this work. The dependence of $\gamma_i(He^+)$ on ion energy observed here is seen to resemble that observed for gas-covered Mo (Fig. 6 of reference 1) and not that for atomically clean Mo. This is the first of several pieces of evidence relating to the state of the target surface.

Retarding potential curves from which electron energy distributions are determined are plotted in Fig. 2. The quantity $\rho=I_S/(I_T+I_S)$ is plotted against the voltage V_{ST} between target and electron collector, corrected for the measured contact potential between the collector and the target. The contact potential measurement[5] is made with the target hot enough to emit electrons thermally and thus strictly gives the correction relative to the *hot* target only. Barring

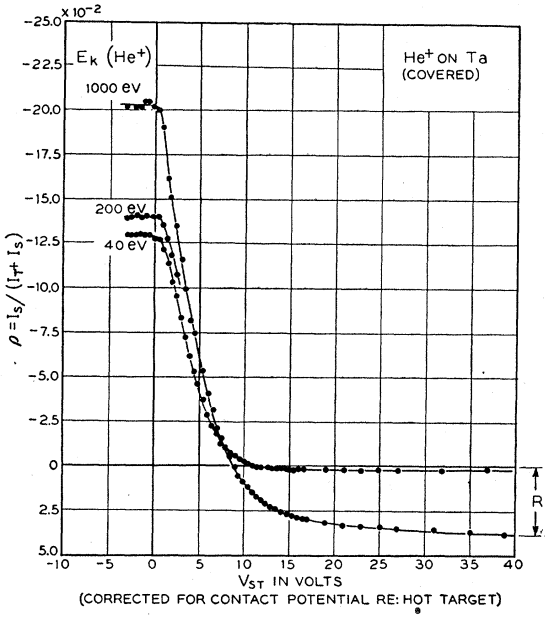

FIG. 2. Retarding potential curves for electrons ejected by He^+ ions of 40-, 200-, and 1000-ev kinetic energy. Note that the abscissa scale is not true retarding potential V_r for the cold target.

extraordinary circumstances, this may also be taken as the contact potential between electron collector and the target immediately after cooling, before an appreciable fraction of a monolayer has been adsorbed upon the surface. Extraordinary circumstances prevail in the case of tantalum, however, a second evidence of which is to be noted in the curves of Fig. 2. The downward break from the value of ρ at $V_{ST}<0$ $(=\gamma_i)$ is seen to occur nearly a volt to the right of the zero axis. This is observed at each ion energy used and represents a behavior at variance with that observed for clean Mo.

In Fig. 3 are plotted the initial portions of retarding potential curves for covered Ta and atomically clean Mo determined with He^+ ions of 200-ev energy. Both are plotted against V_{ST} corrected by the contact

[5] See Sec. VIII of reference 2.

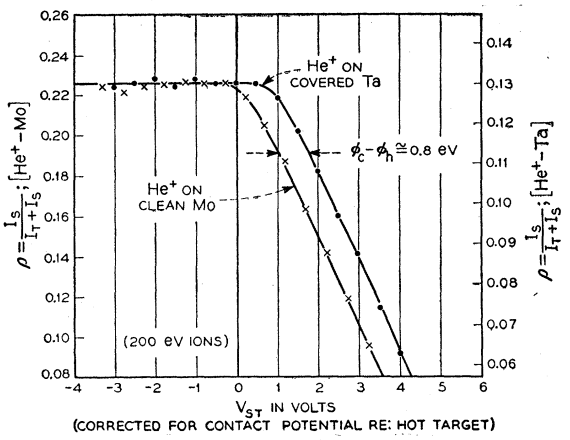

FIG. 3. "Initial" portions of ρ *vs* V_{ST} curves for He^+ ions of 200 ev incident on atomically clean Mo and gas-covered Ta. The abscissa scale has been corrected for contact potential relative to the hot target and represents the true V_r scale for the Mo only. The shift of the Ta curve is caused by the increase of work function of the Ta on cooling as discussed in the text. The ordinate scales have been adjusted in extension to make the slopes of the curves at positive V_{ST} about equal and have been adjusted relative to one another so as to make the horizontal portions at negative V_{ST} colinear.

potential measured relative to the hot target. It is unthinkable that the tantalum curve indicates a measured minimum electron energy in the distribution greater than zero. The finite size of the target relative to the electron collector makes electrons of apparently zero energy appear in the measured distribution, even though, in fact, the actual distribution does not extend

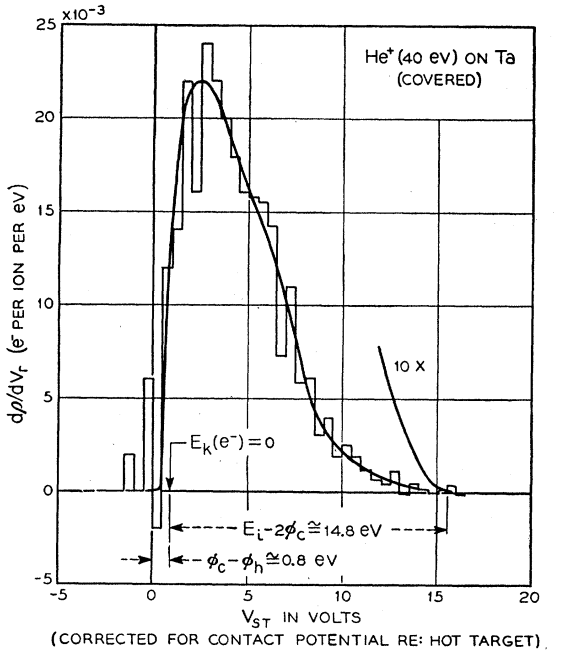

FIG. 4. Plot of $\Delta\rho/\Delta V_r$ obtained from the retarding potential data for electrons ejected by 40-ev He^+ ions. A smoothed $d\rho/dV_r$ curve is drawn through the stepped curve.

to zero energy. One must conclude that since the retarding potential curve is measured with the target at room temperature, the shift of the curve on the V_{ST} scale to be seen in Fig. 3 is the result of an increase in the target work function on cooling. The curve for clean Mo is taken to represent the curve obtainable with a metal whose work function does not alter appreciably on cooling. None of the evidences presented in this paper which indicate the rapid covering of the tantalum on cooling with a surface layer of atoms from within the metal were observed for molybdenum. The small dependence of work function on temperature for a clean metal is not taken into account specifically here. If it were the same for clean Ta and clean Mo, its effect would cancel out of these measurements.

The relative positions on the abscissa scale of the two curves of Fig. 3 is taken to indicate that the work function of the tantalum at room temperature φ_c is *ca* 0.8 ev greater than that of the hot tantalum φ_h. Whether φ_h is the work function φ of atomically clean Ta or not has not been demonstrated. φ_h is probably equal to φ, but if not, is most likely greater than φ. The true retarding potential (V_r), when the tantalum target is at room temperature, is to be obtained by subtracting 0.8 volt from the V_{ST} scale which has already been corrected by the *measured* contact potential.

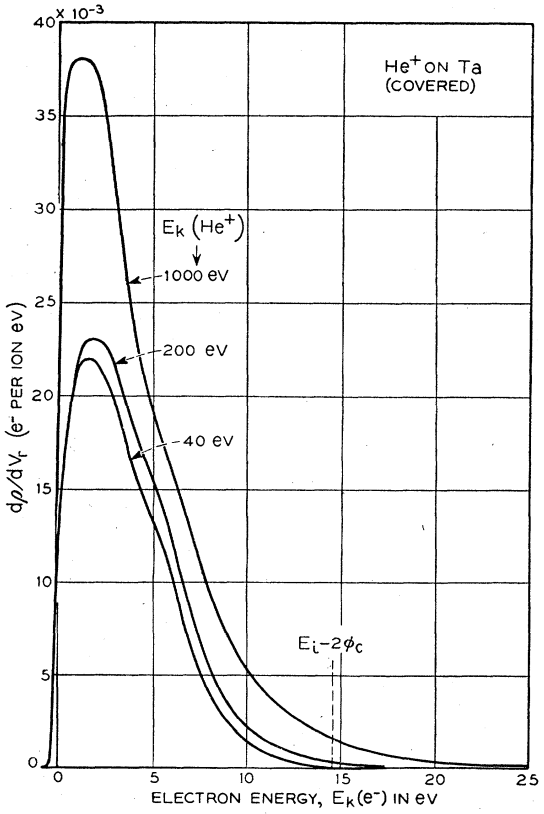

FIG. 5. Kinetic energy distributions of electrons ejected by He^+ ions of 40-, 200-, and 1000-ev kinetic energy. Note that the abscissa scale here has been corrected by contact potential *to the cold target* and is thus shifted by 0.8 volt from those of Figs. 2, 3, and 4.

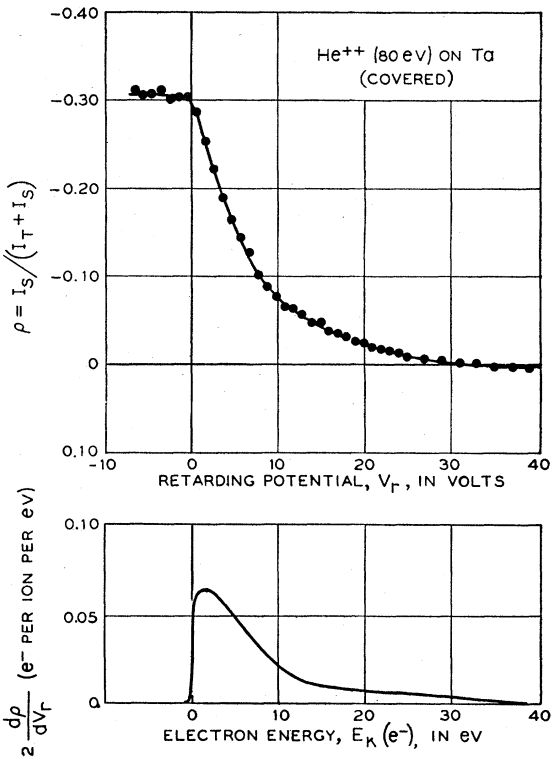

FIG. 6. Retarding potential curve (top) and energy distribution (bottom) for electrons from He^{++} ions of 80-ev energy incident on gas-covered tantalum. Note that for both of these curves the abscissa scale used is the true V_r scale, i.e., the V_{ST} scale corrected by contact potential to the *cold* target.

The electron energy distribution function is obtained from the ρ *vs.* V_{ST} curve by differentiation. This has been done in this work by plotting the $\Delta\rho/\Delta V_r$ curve calculated from the data (the step curve in Fig. 4) and drawing through this a smooth curve (also to be seen in Fig. 4). $d\rho/dV_r$ curves obtained in this manner for each of the energies of He^+ used are shown in Fig. 5 plotted to the true V_r scale, as defined above. The reasons for the small extension of these curves to negative V_r has been discussed in Sec. VI of reference 1. Here again the resemblance of these curves to those for gas-covered Mo is to be noted. Attention is called to the fact that the distribution for $E_k(He^+)=40$ ev contains no electrons of energies greater than the limit $(E_i-2\varphi_c)$ and that the distribution for $E_k(He^+)=1000$ ev does. These facts will be discussed in Sec. V.

In Fig. 6 retarding potential data and electron energy distribution for ejection by He^{++} are plotted.

Many of the conclusions to be drawn from the data presented here are the same as those already drawn in the case of He ions on Mo. They will be only briefly summarized here. Nine points may be made, as follows.

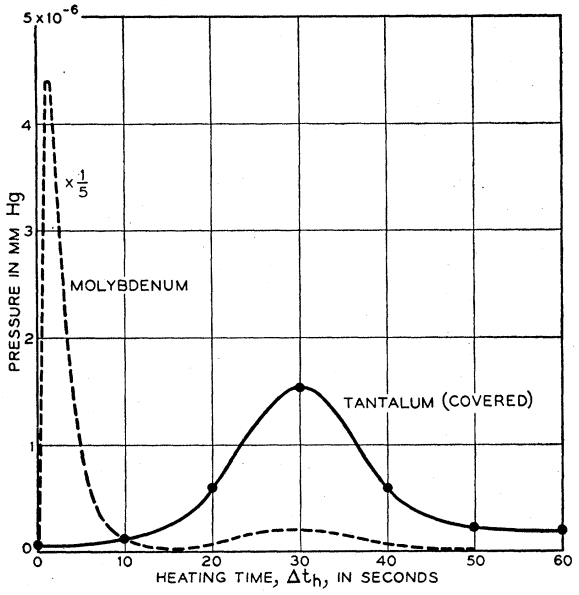

FIG. 7. Plots of pressure *versus* heating time Δt_h, observed for tantalum and molybdenum targets heated to 1750°K. The curve for the molybdenum target is schematic. The maxima in the pressure rise at $\Delta t_h \cong 1$ and 30 sec are designated $(\Delta p)_1$ and $(\Delta p)_2$, respectively. Note that $(\Delta p)_1 = 0$ for the tantalum target.

1. γ_i is remarkably independent of ion kinetic energy (Fig. 1). This is taken to indicate a *potential* ejection mechanism.

2. The quantity $R = I_r/I^i$ (the value of ρ at $V_r \gg 0$) is found to be small relative to γ_i, at least at low ion energy (Fig. 2). I_r specifies the secondary ionic and tertiary electronic currents which flow between target and electron collector as the result of reflection of ions as ions or metastable atoms at the target surface. Thus the smallness of R indicates that essentially every ion decays to the normal atom at the metal surface.

3. The measured value of γ_i is considerably less than 0.5, despite the fact that every ion decays. This is taken to indicate refraction and partial internal reflection at the image barrier of the internal secondary electrons as they attempt to leave the metal.[6] The observed value of γ_i is then determined principally by the probability of the electrons escaping from the metal rather than by the probability of excitation of electrons which is near unity.

4. The electron yields for He^{++}, He^+, and He_2^+ are roughly in the ratio of energy available after neutralization, that is: $\gamma_i(He^{++}):\gamma_i(He^+):\gamma_i(He_2^+) \cong [E_{i2}(He) - 2\varphi_c]:[E_{i1}(He) - \varphi_c]:[E_i^v(He_2) - \varphi_c]$.[7] This result is consistent with the observation that the average energy of electrons ejected by He^+ and He^{++} are roughly equal (see item 9 below).

5. The maximum kinetic energy in the distribution of electrons ejected by slow He^+ ions (40 ev) is, if anything, less than the limit $E_i - 2\varphi_c$ predicted for the direct Auger process (Fig. 2 of reference 1) without any account being taken of energy level shifts when the atomic particle is near the metal surface. This point is discussed again in Sec. V below.

6. Both the γ_i *vs* $E_k(He^+)$ and the $d\rho/dV_r$ *vs* $E_k(e^-)$ curves found here resemble in form those observed for gas-covered tantalum. γ_i is found to rise steadily with $E_k(He^+)$, not to drop first and rise again with increasing $E_k(He^+)$, as was observed with clean Mo. The electron energy distributions are found to be deficient in faster electrons as was found for covered Mo with respect to clean Mo.

7. The quantity R is observed to increase with kinetic energy of the incoming ion indicating greater chance of reflection as an ion or metastable atom as the ion approach velocity increases.

8. Electrons are found to be ejected with velocities in excess of the limit $E_i - 2\varphi_c$, when the incident ion energy is 1000 ev. Here is further evidence of the deficiencies of the published theories in that they neglect energy level shifts near the metal surface.

9. Electrons ejected by He^{++} possess, on the average, little more energy than those ejected by He^+. This is taken to indicate a stepwise decay of He^{++} to normal He, one electron being excited inside the metal per jump. The γ-ratios mentioned in item 4 may also be taken as evidence supporting this view.

Further discussion of the tantalum results as they relate to the state of the target surface is included in Sec. IV, and as they relate to present and proposed theory in Sec. V. There have been published no other studies of electron ejection from Ta by noble gas ions with which the present results may be compared.

IV. STATE OF THE TANTALUM SURFACE

In the results of the electron ejection experiments, we have seen two evidences that the tantalum surface at room temperature is not atomically clean. These are: (1) that the forms of the γ_i *vs* E_k and $d\rho/dV_r$ curves resemble those for gas-covered molybdenum and (2) that the work function of the cold surface appears to be

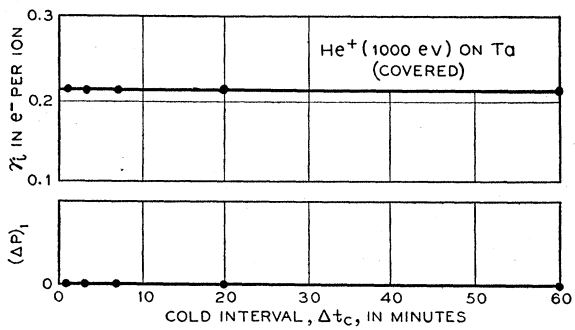

FIG. 8. Plots of γ_i, the electron yield per incident ion, and $(\Delta p)_1$, the pressure rise observed when the tantalum target is heated, as functions of target cold interval. The γ_i-measurements were made with He^+ ions of 1000-ev kinetic energy at the target. Note specific definition of $(\Delta p)_1$ in Fig. 1.

[6] Sec. V and Fig. 7 of reference 1.
[7] This is further discussed in Sec. V of reference 1.

ca 0.8 ev greater than that of the hot surface. Two further results concerned with the state of the tantalum surface are the following: (3) No gas could be removed from the tantalum by heating to 1750°K, and (4) γ_i was observed to be independent of time after cooling from 1750°K.

In the experiment with molybdenum, it was possible to measure the rate of adsorption of residual gases on the target and thus to determine the so-called monolayer adsorption time. This time interval turned out to be sufficiently great to show the molybdenum to be atomically clean to within a few percent for secondary electron emission measurements made within a few minutes after a target flash. This was not possible in the case of tantalum. Although the Ta target was heated to 1750°K as was the Mo, at no time was a pressure rise observed on heating. This result is to be seen in Fig. 7. Despite the fact that the target comes up to temperature in 1 to 2 seconds, it is seen that the pressure begins to rise only after a considerably greater time has elapsed, reaching a peak some 30 seconds after heating commenced. This later pressure rise is the result of evolution of gas from the heavy molybdenum leads to which the thin target ribbon is attached. After passing through the maximum at 30 seconds the pressure drops to a value below 2×10^{-7} mm Hg, where it has been observed to remain with the target hot for as long as 20 minutes. The dashed curve of Fig. 7 represents schematically the p *vs* Δt_h dependence characteristic of a Mo target. Note the large pressure rise in about 1 second as gas is desorbed from the target itself as well as the desorption of gas from the target leads at longer times.

The evidence concerning the variation of γ_i with target cold interval Δt_c is to be found in Fig. 8, in which both γ_i and $(\Delta p)_1$ are plotted as functions of Δt_c. Neither is observed to vary with Δt_c, in remarkable contrast to what was observed with Mo (Fig. 5 of reference 1). γ_i at other ion energies was also found to be independent of target cold interval.

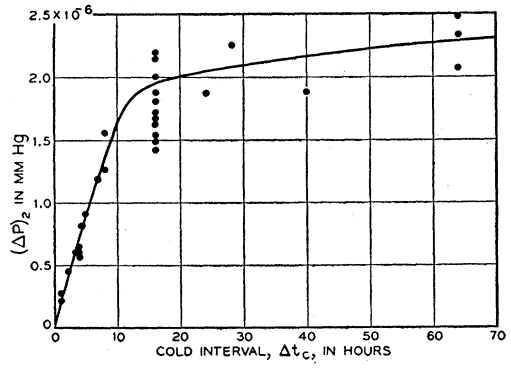

FIG. 9. Plot of $(\Delta p)_2$ *versus* Δt_c for release of adsorbed gas from the target support leads. All the data taken over a period of several weeks are plotted here.

What we now know and are driven to conclude about the state of the tantalum surface is the following. It has a work function when cold *ca* 0.8 ev greater than when hot. Clearly the cold surface differs from the hot surface and must be covered with adsorbed atoms. However, no gas is observed to flash off the surface. Hence, the surface layer must be "swallowed" into the lattice on heating. But the surface condition of the tantalum, when cold, reestablishes itself in less than one minute, the Δt_c value of the first reading of the γ_i-curve of Fig. 8. It is true that one depends here upon a γ_i-measurement which could conceivably be insensitive to the surface condition. This is considered unlikely in view of the observations of changes in γ_i with the adsorption of gas on Mo[1] and on W.[8] Furthermore, one cannot attribute the rapid restoration of the equilibrium surface condition to adsorption from the surrounding residual gas in the apparatus. The arrival rate of gas molecules at the surface is too small. The experimental evidence for this last statement is the $(\Delta p)_2$ *vs* Δt_c-curve of Fig. 9, which shows the adsorption rate on the target supporting leads to correspond to a monolayer adsorption time close to 10 hours.

The evidences from several directions thus appear to point to the following conclusion with respect to the state of the tantalum surface. When cold, it is covered with an equilibrium gas layer. This layer is absorbed into the body of the metal on heating to 1750°K reducing the surface work function by *ca* 0.8 ev. The surface layer is re-established rapidly on cooling by the "squeezing out" of the absorbed gas onto the surface again. Presumably the continued periodic heating has brought about a state of equilibrium such that no further gas need be adsorbed from the surroundings. If φ_h is taken as equal to $\varphi(\text{Ta})=4.12$ ev, φ_c is approximately 4.9 ev.

The behavior of tantalum observed in this work is in accord with what is known of the reaction of gases with incandescent tantalum. Andrews,[9] for example, reports that N_2 is readily absorbed by Ta at 2100°K, slowly below 1600°K. O_2 is taken up readily at 1000°K and with extreme rapidity at 1800°K. H_2O, on the other hand, is decomposed above 1400°K, according to Andrews, the O_2 being absorbed and the H_2 evolved. The residual gas in the present apparatus consists predominantly of CO, which may presumably be taken to behave with respect to adsorption much like N_2. O_2 has never been observed with the mass spectrometer. From the fact that no gas is evolved when the Ta is heated and Andrews' result that H_2 is evolved when H_2O decomposes, it may be concluded that little H_2O is present in the background gas, although it was observed in the early stages of the evacuation procedure.

[8] Work done on the adsorption of the common gases, including N_2 and CO, on *W* and its effect on the electron ejection by ions is to be published soon. See H. D. Hagstrum, Phys. Rev. **89**, 338 (1953).

[9] M. R. Andrews, J. Am. Chem. Soc. **54**, 1845 (1932).

V. DISCUSSION OF THEORY

In the published literature there are wave mechanical theories which deal with two types of possible potential ejection processes.[10] These processes are (1) the direct neutralization of the ion to the normal state of the atom accompanied by the excitation of an internal secondary electron (called here the direct process) and (2) the resonance neutralization of the ion to the metastable state followed by the decay of the metastable atom with excitation of an internal secondary electron (called here the two-stage process). The calculations of the transition probabilities involved have all neglected shifts of atomic energy levels near the metal surface. In the present work and the earlier molybdenum work,[1] there are definite violations for fast ions of the electron kinetic energy limits expected on the basis of no energy level variation.

The treatment of electronic transitions in diatomic molecules is suggestive of a manner of description in the present case which lends itself to the inclusion of the energies of interaction between the metal and the atomic particles involved. One calculates, or estimates where necessary, the potential energy of the ion, metastable atom, and normal atom as a function of distance outside the metal surface. Such potential energy curves are placed properly with respect to each other on an energy-distance plot by consideration of the energy transformations in isoelectronic systems necessary to go from one state to another with the atomic particle removed to an infinite distance. The electronic transitions involved in potential ejection processes are then described as jumps between these potential curves which obey the Franck-Condon principle. The probability of a transition at a given distance from the metal may be considered to be given, to order of magnitude at least, by the wave mechanical theories which neglect level shifts. This approach is most useful in determining whether a process (resonance neutralization, for example) can or cannot occur at a certain atom-metal distance and what are the energy limits to be expected for electrons ejected by the Auger processes listed above.[11]

The forces considered in drawing potential energy curves are (1) the image force of attraction for ions, (2) the van der Waals forces of attraction between the metastable atom or the normal atom and the metal, and (3) the repulsive forces which set in at close approach. The image force can be calculated exactly. The van der Waals attractions have been calculated by the formula of Prosen and Sachs.[12] The repulsive forces must be estimated. The reasonable assumption has been made, however, that these forces *may* become appreciable at distances from the metal which increase with the diameter of the atomic particle in question. This assumption has been found adequate to indicate significant differences between the energy limits to be expected for electrons ejected by the direct *versus* the two-stage ejection mechanisms.

The conclusions with respect to the energy limits of electrons resulting from the direct and the two-stage ejection processes are the following, stated here without proof. The direct process is expected to yield electrons which for sufficiently slow ions have energies outside the metal which cannot exceed the limit $E_i-2\varphi$. The two-stage process, on the other hand, is expected to yield electrons whose energies do exceed the limit $E_x-\phi$ calculated for this process neglecting level shifts. It may be stated that in the work on noble gas ions on W, mentioned in Sec. I of this paper as being in preparation for publication, there are to be found examples of both of the cases listed. As the approach velocity of the ion is increased, an increasing proportion of the electronic transitions resulting in secondary electron emission occur very close to the metal surface where the energy levels are most likely quite diffuse. This possibility is called upon to account, at least in part, for electrons ejected by faster ions (1000 ev) which possess energies in excess of the limits given in either case.

In the light of the theory sketched above there are two points of interest in the case of He^+ on Ta. These are: (1) Can He^+ be neutralized to the metastable level He^m, making the two-stage ejection process possible, and (2) are the observed energy limits for slow ions (40 ev) consistent with the result of point (1) and the theoretical conclusions with regard to the energy limits to be expected from the two types of ejection processes? Interest in the answers to these questions is heightened because they are intimately bound up with the value of the work function of the tantalum surface and must be consistent with the conclusions concerning the state of the tantalum surface already indicated (Sec. IV).

We consider first the possibility of resonance neutralization to the metastable level. This process may be written thus:

$$He^+ + e^-_{Ta}(-\alpha) \rightarrow He^m, \qquad (1)$$

where $-\alpha$ is an energy below the vacuum level which puts e^-_{Ta} in the conduction band, i.e., $\varphi<\alpha<W_a$. In addition, α must have the value which makes the energies represented on the two sides of Eq. (1) equal. Neglecting the energies of interaction of He^+ and He^m with Ta, it is apparent that $\alpha=\epsilon$ is the value which meets this criterion. Thus, on this simple picture the process of Eq. (1) can occur if $\varphi<\epsilon<W_a$ and cannot if $\epsilon<\varphi$.

Including the energies of interaction of the atomic particles with the metal surface, the energy balance demanded by Eq. (1) and the Franck-Condon principle, taking the energy level of the system $He^+ + e^-_{Ta}(-\varphi)$

[10] The results of these theories have been summarized in Sec. II of reference 1.

[11] Results of this potential curve theory were mentioned briefly in Sec. VII of reference 1.

[12] Equation (20) of E. J. R. Prosen and R. G. Sachs, Phys. Rev. **61**, 65 (1942).

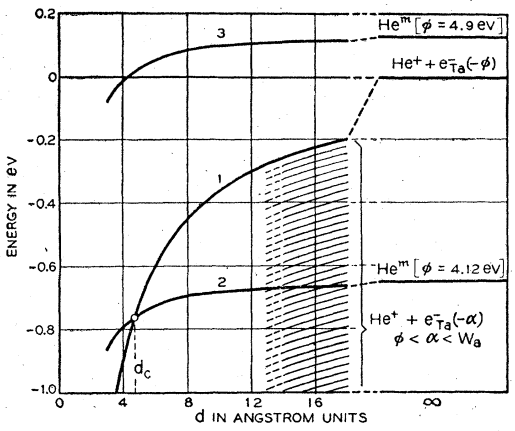

FIG. 10. Potential energy diagram for the case of resonance neutralization of He^+ to He^m at a tantalum surface. Curves are drawn representing the situation for atomically clean Ta (φ=4.12 ev) and for the covered Ta encountered in the experimental work ($\varphi=\varphi_c\cong$4.9 ev). Discussion of the conclusions drawn is to be found in Sec. V of this paper.

as zero, is the following:

$$E(\mathrm{He}^+-\mathrm{Ta})-(\alpha-\varphi)=E(\mathrm{He}^m-\mathrm{Ta})-(\epsilon-\varphi), \quad (2)$$

or

$$\alpha=E(\mathrm{He}^+-\mathrm{Ta})-E(\mathrm{He}^m-\mathrm{Ta})+\epsilon. \quad (3)$$

The Franck-Condon principle must be applied here, because the interaction energies involved are functions of the metal-atom distance d. The Franck-Condon principle, in this case, states that the position and momentum of the atomic particle relative to the metal are essentially unaltered during the electronic transition represented by Eq. (1). Only if this is true can one insert expressions for $E(\mathrm{He}^+-\mathrm{Ta})$ which involve the distance d and calculate α on a quasi-equilibrium basis as a function of d.

For $E(\mathrm{He}^+-\mathrm{Ta})$ we use the image potential energy $-e^2/4d$, and for $E(\mathrm{He}^m-\mathrm{Ta})$, the van der Waals interaction energy, $-[\alpha_m e^2\pi k_{\max}{}^2\ln(2k_{\max}d)]/(2\pi)^3d^2$, calculated by Prosen and Sachs.[12] Numerical values used are specified in Table I. Insertion of these expressions into Eq. (3) yields

$$\alpha=-\frac{e^2}{4d}+\frac{\alpha_m e^2\pi k_{\max}{}^2\ln(2k_{\max}d)}{(2\pi)^3d^2}+\epsilon. \quad (4)$$

As d decreases from large values toward zero, α decreases since the image potential term $-e^2/4d$ predominates. When α reaches the value φ, the work function of the metal, the neutralizing electron is removed from the top of the conduction band. The distance d_c at which this takes place represents a critical distance beyond which resonance neutralization is possible and within which it is not. For $d<d_c$, $\alpha<\varphi$ in which region the energy levels are not populated (neglecting the small population above the Fermi level at temperatures above absolute zero). If the resonance neutralization has occurred at $d>d_c$, it is possible, however, for the metastable atom so formed to be ionized at $d<d_c$.[13]

The relationships discussed above are conveniently shown in the potential energy diagram of Fig. 10. Here the potential energies of the isoelectronic systems represented on each side of Eq. (1) are plotted against the distance, d, between the metal surface and the atomic particle. These potential energies are specified in Eq. (2). Curve 1 represents the energy of the system $\mathrm{He}^+ + e^-_{\mathrm{Ta}}(-\varphi)$ as a function of d. This level lies below that of $\mathrm{He}^+ + e^-_{\mathrm{Ta}}(-\varphi)$ at $d=\infty$, taken as zero, by the image potential $-e^2/4d$. Below curve 1 there lies a continuum of potential curves representing the levels $\mathrm{He}^+ + e^-_{\mathrm{Ta}}(-\alpha)$, $\varphi<\alpha<W_a$, which extends to a level W_i below curve 1. Curve 2 represents the level of the metastable atom He^m relative to $\mathrm{He}^+ + e^-_{\mathrm{Ta}}(-\varphi)$ at $d=\infty$. Its variation with distance is given relative to the assumed zero level by $E(\mathrm{He}^m-\mathrm{Ta})-(\epsilon-\varphi)$. Curve 2 is drawn for $\varphi=\varphi(\mathrm{Ta})=4.12$ ev, curve 3 for $\varphi=\varphi_c=4.9$ ev.

The Franck-Condon principle permits transitions from $\mathrm{He}^+ + e^-_{\mathrm{Ta}}(-\alpha)$ to He^m only at crossing points of the corresponding potential curves. It is clear from Fig. 10 that curve 2 crosses some curve in the continuum below curve 1 at all $d>d_c$. Curve 3 crosses no curve belonging to the family of states $\mathrm{He}^+ + e^-_{\mathrm{Ta}}(-\alpha)$, $\varphi<\alpha<W_a$. Thus, if the conclusions concerning the work function of the tantalum already arrived at are correct, $\varphi=\varphi_c$ and the resonance neutralization process cannot occur at any distance d. Hence, the only potential ejection process possible for covered tantalum is the direct process for which, at low incoming ion velocity, the electron energies should not exceed $E_i-2\varphi_c$. That this is true is to be seen in Fig. 5 [$E_k(\mathrm{He}^+)=40$ ev].

It should be noted that the resonance neutralization of He^+ to He^m at an atomically clean Ta surface would be possible only if the transition probability has become appreciable before the ion crosses the critical distance d_c. Sternberg[14] has recently calculated 4 to 5A as the distance at which it becomes highly probable that a 10-ev He^+ ion will be neutralized. Thus resonance neutralization of He^+ at an atomically clean Ta surface should just be possible. However, the uncertainties in the van der Waals interaction term used here should not be forgotten.

Finally, it should be remarked that the direct process predicts a minimum electron energy of $E_i-2W_a\cong$4.0 ev on the basis of no energy level shifts near the metal surface. Consideration of the process in more detail shows this limit to be reduced by energy level shifts

[13] L. J. Varnerin, Jr. (private communication) has found independently that inclusion of the image potential in the consideration of the resonance neutralization process yields the critical atom-metal distance, with respect to which the process may or may not proceed as described here.

[14] D. Sternberg (private communication).

near the metal. Furthermore, the finite size of the target precludes observation of a minimum energy greater than zero on geometrical grounds.

The discussion of theory included here is admittedly sketchy. It is meant to show the consistency of the theoretical results with the conclusions concerning the state of the tantalum surface and its work function demanded by the experiment. A detailed account of the theory, including conclusions stated here without proof, is forthcoming.

The author wishes to acknowledge with thanks the discussions with his colleagues, J. A. Hornbeck, K. G. McKay, J. P. Molnar, and A. H. White, the efforts of H. W. Weinhart in design and supervision of construction of the experimental apparatus, and the technical assistance of F. J. Koch.

PHYSICAL REVIEW VOLUME 91, NUMBER 3 AUGUST 1, 1953

Reversible Bleaching of a Band in the Absorption Spectrum of Diamond

PETER PRINGSHEIM
Chemistry Division, Argonne National Laboratory, Lemont, Illinois
(Received April 13, 1953)

When diamonds which show the absorption band in the near ultraviolet, characteristic of blue fluorescing samples, are exposed to neutron bombardment, a continuous absorption slowly rising toward shorter wavelength is superimposed upon the band. Heating such a diamond to temperatures between 300° and 600°C decreases the continuous absorption and the structure of the band becomes appreciably sharper. Subsequent exposure to light greatly reduces the height of individual peaks in the band, while the continuous absorption at shorter wavelengths is increased. Renewed heating restores the sharp structure of the band and the cycle can be repeated at will. Heating the crystal to 750°C brings the crystal very nearly back into the state before neutron bombardment in which the reversible bleaching cannot be observed. A similar band accompanies the sharp line at 503 mμ that is produced in the absorption spectrum of diamonds by neutron bombardment and heat. The structure of this band is also altered by heating to various temperatures but is not affected by absorption of light.

MOST diamonds of the so-called type I show in their absorption spectra a sharp line at 415.2 mμ and an adjoining band with a number of peaks in the range from 405 to 350 mμ. It has been mentioned in a preceding paper[1] that under certain conditions the intensity distribution within this band can be altered appreciably and reversibly by heating a diamond in the dark to temperatures between 300 and 500°C and then exposing it to violet or near ultraviolet radiation. The phenomenon had been observed only with a diamond which had previously been subjected to neutron bombardment in the Argonne heavy water pile. However, since the band was present in the absorption spectrum before this treatment, it seemed probable that even then it would have exhibited the same behavior which might be connected with the well-known thermoluminescence properties of many diamonds.

In more recent experiments, several diamonds were investigated in which the line and band in the neighborhood of 400 mμ in the absorption spectra before irradiation had a much greater intensity than in the earlier sample. Moreover, the spectra were recorded at the temperature of liquid nitrogen at which temperature the structure of the band is much better resolved than at room temperature. Figure 1, curve a represents the absorption spectrum from 800 to 300 mμ of one of the new diamonds (D46) before any treatment. The line at 415.2 mμ is somewhat distorted on the curves of Fig. 1 because the scanning speed of the recording spectrophotometer was too great for the high intensity and sharpness of the line. Curve a in Fig. 2 represents the region from 420 to 300 mμ of the same spectrum with a tenfold slower scanning speed. The relative intensities of the line and the various band peaks are shown with much better accuracy in this figure.[2] Repeated heating of the diamond to temperatures between 300 and 650°C and subsequent exposure to light did not alter the spectrum in the least. The same result was obtained with another sample (D52). Curves b in Figs. 1 and 2 represent the absorption spectrum of the diamond D46 after 20 hours exposure to neutron bombardment. The absorption spectrum is characterized by a broad band in the orange and a strong increase of absorption below 500 mμ. Since the maximum transmission is located in the neighborhood of 500 mμ, the crystal acquired the well-known blue-green color in transmitted light. The nearly straight line c, obtained as the difference between curves b and a in Fig. 2, proves that, at least in this spectral region, the effect of the pile exposure consists only in the super-

[1] P. Pringsheim and R. Voreck, Z. Physik **133**, 2 (1952).

[2] On spectrograms obtained by several investigators with spectrographs of higher resolving power, additional fine structure appears in the band, of which only a trace can be recognized in the curves of Figs. 2 and 3. [See P. G. N. Nayar, Proc. Indian Acad. Sci. **A15**, 293 (1942); A. Mani, Proc. Indian Acad. Sci. **A19**, 231 (1944).]